RSC Advances

ROYAL SOCIETY OF CHEMISTRY

www.rsc.org/advances

Cite this: DOI: 10.1039/c0xx00000x

www.rsc.org/xxxxxx

ARTICLE TYPE

Mononuclear manganese (III) complexes of bidentate NO donor Schiff base ligands: synthesis, structural characterization, magnetic and catecholase studies

Arpan Dutta[a], Surajit Biswas[a], Malay Dolai[a], Bikash Kumar Shaw[b], Abhishake Mondal[a], Shyamal Kumar Saha[b] and Mahammad Ali*[a]

Received (in XXX, XXX) Xth XXXXXXXXX 200X, Accepted Xth XXXXXXXXX 200X

DOI: 10.1039/b000000x

Abstract:

We have synthesized four mononuclear manganese(III) complexes (**1**-**4**) of four closely related bidentate NO donor Schiff-base ligands, out of which three (**2**-**4**) were structurally characterized. Crystal structure determination reveals that all these complexes are in octahedral geometries. Magnetic studies have been carried out on complexes **2**, **3** and **4** in the temperature range 2–300 K under a magnetic field of 0.1 T which yielded negative ZFS parameters as –2.96, –3.51 and –3.72 cm^{-1} respectively. The catecholase activities of complexes **1–4** have been investigated following the oxidation of 3,5-di-*tert*-butylcatechol (3,5-DTBC) to 3,5-di-*tert*-butylbenzoquinone (3,5-DTBQ) with molecular oxygen in DCM at 25 °C which were found to follow the Michalis-Menton type relation giving the highest TON (K_{cat}) for the so far reported Mn(III) complexes.

Introduction:

It is now well established that a number of Mn-containing biomolecules are found to contain manganese as mononuclear (superoxide dismutase[1] and manganese dioxygenase[2]), dinuclear (catalases,[3-7] ribonucleotide reductase,[8] arginase[9]) and also as tetranuclear (oxygen evolving complex[10]) species. A significant advancement has been achieved in the biomimetic structural and functional modelling of manganese containing enzymes by the synthetic chemists and biochemists which have added a wealth of knowledge to our understanding of various aspects of manganese cluster chemistry with respect to structural, electrochemical and magnetic properties. In addition, these structural or functional models are also important in catalyzing a number of organic reactions[11-15] Though structural and functional models of manganese containing metalloenzymes have been extensively explored[16,17] this area is yet under continuous development.[18,19]

Catechol oxidase (CO) is a member of the type-III copper proteins[20] which catalyzes exclusively the oxidation of catechols to the corresponding quinones, highly reactive intermediates that undergo auto-polymerization to produce melanin, a brown pigment responsible for protecting damaged tissues against pathogens and insects of the higher plants. Although CO is believed to be a copper containing protein and many dicopper complexes are found to act as successful models for such metalloenzymes; there are only few reports where manganese [21-35] complexes were found to display such activities as well, despite the fact that no such native enzymes having metal ions other than copper is known. In these complexes tetradentate tripodal ligands, several pyridine derivatives, azametallacrown and compartmental Schiff base ligands have been utilized but there is no repot on the mononuclear octahedral Mn(III) complexes of bidentate Schiff base ligands that display catecholase activities. Therefore, design and synthesis of functional model of CO containing metal ions other than copper, say manganese, seems to be interesting and at the same time challenging.

High-spin manganese(III) complexes with ^5D ground term splits in octahedral crystal fields into $^5T_{2g}$, and ^5E_g, terms. Non-cubic

[a] *Department of Chemistry Jadavpur University, Kolkata 700 032, India; Fax: 91-33-2414-6223, E-mail: mali@chemistry.jdvu.ac.in*

[b] *Department of Materials Science, Indian Association for the Cultivation of Science, Kolkata - 700 032, India*

symmetry and/or Jahn-Teller distortions are responsible to lift the oribtal degeneracy of the ^5E_g, ground term to orbital singlet lowest, either $^5A_{1g}$ or $^5B_{1g}$, (in D_{4h} symmetry). The spin degeneracy of the ground state is further lifted by spin-orbit coupling to give the so-called zero-field splitting (ZFS).

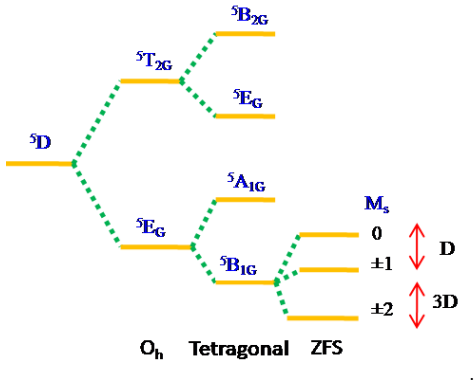

The exact nature of the ground state depends critically on the symmetry of the ligand field and the nature of metal ion. If the $d_{x^2-y^2}$ orbital is unoccupied, then the complex is expected to be axially elongated, with the $^5B_{1g}$ level lying lowest. Such a ground term is expected[37] to have principal susceptibilities in the order $K_{||} > K_{\perp}$, and hence D will be negative. Conversely, compression of the octahedron results in the $^5A_{1g}$, lying lowest with positive D.

The zero-field splitting in Mn(III) is typically of the order of a few wavenumbers, and so the magnetic properties are expected to be Curie-like and close to spin only value (4.90 μ_B), except at very low temperatures where a rapid decrease in μ_{Mn} occurs. In fact, a number of studies on hexacoordinated Mn(III) Schiff-base complexes showed that these complexes displayed Curie-like behaviour in the temperature range 80-300 K with magnetic moments of about 4.90 μB.[38-40] Owing to small size of the ZFS, together with the possibilities of weak magnetic exchange, exact interpretation of the data was not always possible, and the possibility of relatively large errors in the magnitude of such interactions existed. More recently, a number of structural studies on Mn(III) Schiff-base complexes have been reported,[41] mostly showing the presence of quite appreciable distortions about the Mn(III) center.Therefore, axially elongated configuration attracted considerable attention in the search for new Mn(III) SIMs with negative *D* values. In the present paper we are going to describe the catecholase activities and magnetic properties of some monomeric octahedral Schiff-base complexes of the type $[Mn(NO)_3]$.

Experimental Section

Materials and reagents

The starting materials for the synthesis of the ligand H_2L^i (**i** =1, 2, 3, and 4) like 5-Bromo-salicylaldehyde, hydroxyl-amine hydrochloride, Na_2SO_4, tetrabutylammonium hydroxide, sodium azide, $Mn(ClO_4)_2.6H_2O$ are of reagent grade and used as received. Solvents like methanol, diethylether, dichloromethane (DCM), acetonitrile were of reagent grade and dried before use.

Physical measurements

Elemental analyses were carried out using a Perkin–Elmer 240 elemental analyzer. Infrared spectra (400–4000 cm^{-1}) were recorded from KBr pellets on a Nickolet Magna IR 750 series-II FTIR spectrophotometers. ^{1}H-NMR spectra were recorded in $CDCl_3$ on a Bruker 300 MHz NMR Spectrophotometer using tetramethylsilane (δ = 0) as an internal standard. UV-Vis spectra and kinetic studies were performed on Agilent 8453 UV-Vis spectrophotometer.

Crystallography

Single crystal X-ray data of **2-4** were collected at room temperature on a Bruker SMART APEX-II CCD diffractometers using graphite monochromated MoK_α radiation (λ = 0.71073Å). Data integration and reductions were processed with SAINT+ software.[42] Structures were solved by the direct method and then refined on F^2 by the full matrix least square technique with SHELX-97 software.[43] The structures were solved by direct methods and refined by a full-matrix least-squares method on F^2 using the SHELXTL crystallographic software package.[43] The crystallographic data for **2-4** are given in **Table 1**.

Magnetic Measurements

Magnetic measurements were performed using a Quantum Design SVSM (Squid-Vibrating Sample Magnetometer) magnetometer. The static susceptibility measurement were performed in 300-1.8 K temperature range with an applied field of 5 kOe. Measurement of magnetization at different fields and at a given temperature confirm the absence of ferromagnetic impurities. Data were corrected for the sample holder and diamagnetism was estimated from Pascal constants.

Syntheses and characterization

Preparation of Schiff Base Ligands

All four ligands (**HL^1**-**HL^4**) were synthesized following the same procedure as described below in details for **HL^1**, except using the appropriate aldehyde and amine.

Synthesis of ligand HL^1

0.136 g (1mmol) of 2-hydroxy-5-methyl benzaldehyde was dissolved in 20 mL ethanol to which 0.110g (1mmol) of

benzylamine was added drop wise and the solution was refluxed for 3-4 hours. It was then cooled and solvent was removed under reduced pressure to get solid product which was recrystallized from MeOH to get pure product. This protocol was adopted for the synthesis of other related ligands viz. **HL²**, **HL³** and **HL⁴**.

Analyses

HL¹ : ^{1}H- NMR: δ in ppm 2.247 (3H, s, -CH_3), 4.73 (2H, s, -CH_2), 6.7- 7.3 (8H, m, aromatic protons), 8.45 (1H, s, -N=CH), 13.41 (1H, s, -OH). ^{13}C-NMR**:** δ in ppm 18.96 (s, Me Carbon), 62.20 (s, C7), 116.36- 159.41 (m, aromatic carbons), 165.94 (s, C8)**.** Elemental analysis: Calculated, C, 80.00; H, 6.67; N, 6.22; Found, C, 81.20; H, 6.33; N, 6.41

HL² : ^{1}H-NMR: δ in ppm 4.82 (2H, s, -CH_2), 6.85- 7.40 (8H, m, aromatic protons), 8.35 (1H, s, -N=CH), 13.42 (1H, s, -OH) **.** ^{13}C-NMR: δ in ppm 62.99 (s, C7), 109.94- 160.11 (m, aromatic carbons), 164.20 (s, C8). Elemental analysis: Calculated, C, 57.93; H, 4.14; N, 4.83; Found, C, 58.32; H, 4.39; N, 5.08

HL³: ^{1}H-NMR: δ in ppm 2.36 (3H, s, -CH_3), 4.77 (2H,s, -CH_2), 6.85- 7.40 (7H, m, aromatic protons), 8.31(1H, s, -N=CH), 13.49 (1H, s, -OH) ^{13}C-NMR: δ in ppm 21.13 (s, Me Carbon), 62.77 (s, C7), 109.99- 160.29 (m, aromatic carbons), 164.07 (s, C8). Elemental analysis: Calculated, C, 59.21; H, 4.61; N, 4.61; Found, C, 60.02; H, 4.35; N, 5.25

HL⁴: ^{1}H-NMR: δ in ppm 4.78 (2H, s, -CH_2), 6.87- 7.43 (7H, m, aromatic protons), 8.36 (1H, s, -N=CH), 13.25 (1H, s, -OH). ^{13}C-NMR: δ in ppm 62.34 (s, C7), 110.08 - 159.99 (m, aromatic carbons), 164.54 (s, C8)**.** Elemental analysis: Calculated, C, 51.77; H, 3.39; N, 4.31; Found, C, 52.52; H, 3.63; N, 5.02

Preparation of complexes 1-4

All complexes were synthesized following the same procedure as described below in details for complex **1**. Bright amorphous solid product was obtained for **1** while shiny single crystals, suitable for single crystal X-ray diffraction were obtained for complexes **2-4**.

Preparation of [Mn(L¹)₃] (1)

3.0 mmol (0.87g) ligand (HL^1) was dissolved in minimum volume of acetonitrile. To this solution an equimolar amount of (0.303 g) TEA (triethylamine) was added followed by 1 mmol (0.254 g) $Mn(ClO_4)_2.6H_2O$. It was then refluxed for 1 hour. The resulting greenish brown solution was cooled to room temperature, filtered and kept in rack where upon dark brown amorphous solid product was obtained within 2-3 days. Yield:0.472g (65%)

Elemental analyses

[Mn^{III}(L¹)₃] (**1**): $C_{45}H_{42}MnN_3O_3$ (M.W= 727.77); ESI-MS(+ve):M+H$^+$=728.81, Elemental analysis: Calculated, C, 74.27; H, 5.82; N, 5.77; Found, C, 75.10; H, 5.45; N, 5.12.

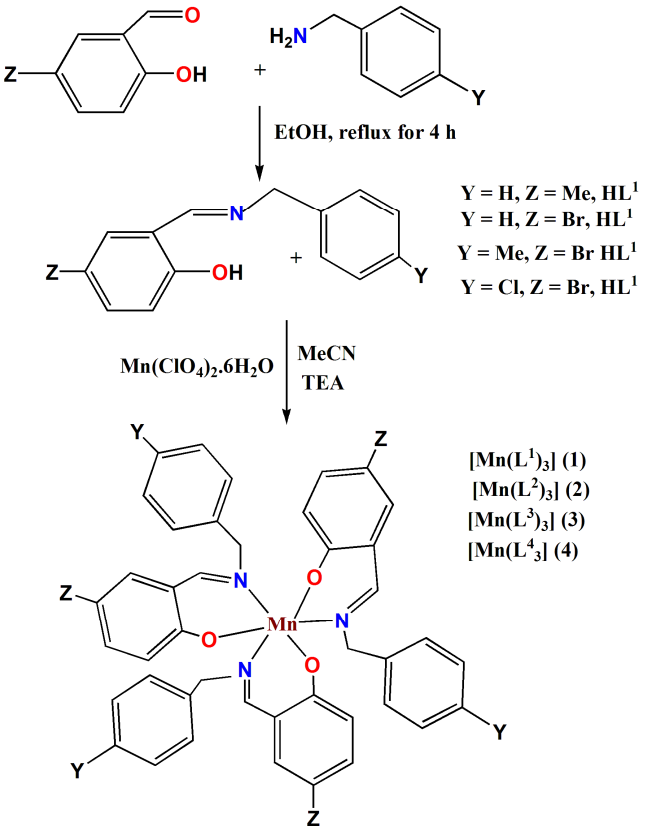

Scheme-1: Schematic presentation of preparation of complexes **1-4**.

[Mn^{III}(L²)₃] (**2**): Color: Dark brown,$C_{42}H_{33}Br_3MnN_3O_3$ (M.W= 922.35); Yield: 0.599g (65%), Calculated, C, 54.68; H, 3.60; N, 4.56; Found, C, 55.38; H, 3.85; N, 4.95

[Mn^{III}(L³)₃] (**3**): Color: Dark green, $C_{45}H_{39}Br_3MnN_3O_3$ (per unit cell)(M.W= 964.43); Yield: 0.655g (68%), Calculated, C, 56.04; H, 4.08; N, 4.36; Found, C, 56.54; H, 4.39; N, 4.77

[Mn^{III}(L⁴)₃] (**4**): Color: Dark Brown, $C_{42}H_{30}Br_3Cl_3MnN_3O_3$ (M.W= 1025.68); Yield: 0.717g (70%), Calculated, C, 49.18; H, 2.95; N, 4.10; Found, C, 50.11; H, 3.15; N, 4.32.

Kinetic studies

All kinetic experiments were carried out under pseudo-first-order conditions, with the Mn(III) complexes as the minor component. All measurements were performed in an Agilent diode-array UV-Vis spectrophotometer. Detail kinetic procedures involve the preparation of stock solutions of complexes (1.0 x 10^{-3} M) and the substrate, 3,5-DTBC, at higher concentrations in pure DCM. From this stock solutions a set of 12 solutions of [3,5-DTBC] = 0.0001-0.01 M were prepared. A 2 ml portion of each solution was pipetted out into a quartz cell and equilibrated for 15 min at 25 ◦C by inserting into the shell holder which is attached to a

peltier temperature controller system. Now 20 µL of stock solution of the complex was added to it to achieve the ultimate concentration of the complex 1.0 x 10^{-5} M.

Table 1. Crystal Data and Details of the Structure Determination

Formula	$C_{42}H_{33}Br_3MnN_3O_3$	$C_{90}H_{79}Br_6Mn_2N_6O_6$	$C_{42}H_{30}Br_3Cl_3MnN_3O_3$
Formula Weight	922.35	1929.87	1025.68
Crystal System	Triclinic	Triclinic	Triclinic
Space group	P-1 (No. 2)	P-1(No. 2)	P-1 (No.2)
a, b, c [Å]	8.246(2) 12.765(4) 18.256(6)	11.5135(4) 14.5392(6) 25.8603(10)	8.8296(15) 12.345(2) 20.440(4)
α, β, γ [°]	70.607(9) 84.283(9) 84.456(8)	103.534(3) 90.011(3) 90.013(3)	76.581(5) 85.576(6) 70.170(5)
V [$Å^3$]	1799.5(9)	4208.7(3)	2038.7(6)
Z	2	2	2
D(calc) [g/cm^3]	1.702	1.523	1.671
μ(MoK_α) [/mm]	3.743	3.205	3.503
F(000)	920	1938	1016
Crystal Size [mm]	0.08 x 0.10 x 0.12	0.09 x 0.15 x 0.23	0.10 x 0.12 x 0.20
Temperature (K)	120	296	120
Radiation [Å MoK_α]	0.71073	0.71073	0.71073
θ_{min}, θ_{max} [°]	1.7, 25.7	0.8, 27.5	1.8, 24.8
Dataset	-6: 10 ; -14: 14 ; -21: 20	-14: 14 ; -18: 18 ; -33: 33	-6: 10 ; -14: 14 ; -24: 24
Tot., Uniq. Data, R(int)	11577, 6805, 0.030	64441, 19368, 0.154	13165, 6902, 0.032
Observed data [I > 2.0 σ(I)]	4184	5262	4265
N_{ref}, N_{par}	6805, 469	19368, 997	6902, 496
R, wR_2, S	0.0390, 0.1275, 0.98	0.0804, 0.1650, 0.992	0.0689, 0.1786, 1.01

Results and Discussion

Synthesis and Structural descriptions of complexes 2-4

Bidentate NO donor ligands **HL^i** (**i**=1-4) were synthesized by the simple Schiff base condensation between appropriate aldehydes and amines in MeOH under refluxing conditions. All the four Mn(III) complexes were synthesized by the reaction between $Mn(ClO_4)_2.6H_2O$ and appropriate ligand in MeCN at ambient temperature which afford single crystals suitable for X-ray diffraction studies with the exception of complex **1**. Several trials to get single crystals of **1** were not successful.

The single crystal X-ray diffraction studies showed that complexes **2**-**4**, depicted in **Figs. 1-3**, are crystallized in *triclinic* system with space group *P-1*. All these complexes are monomeric in nature surrounded by three bidentate NO donor Schiff base ligands. The central manganese atom in each complex is in +3 oxidation state. In case of complexes **2** and **4** there are only one complex unit in the unit cell and the Mn atoms are coordinated by N1, O1, N2, O2 and N3, O3 atom from three ligands while in complex **3** two complex species (**A** and **B**) are p

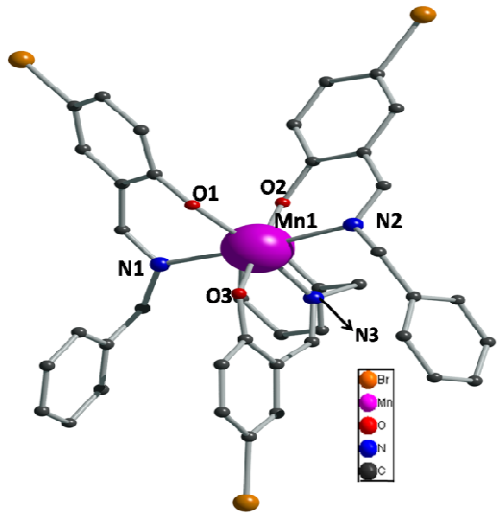

Fig. 1: The molecular view of complex **2**. All H-atoms are omitted for clarity.

resent in the unit cell. In **A** the central manganese(III) ion (Mn1) are coordinated by N1, O1, N2, O2 and N3, O3 and Mn2 atom in **B** is coordinated by N4, O4, N5, O5 and N6, O6, which differ only in bond angles and bond lengths. Mn-O_i distances fall in the range 1.858-1.930Å for **2**, 1.877-1.908Å (**A**) and 1.881-1.929Å (**B**) for **3**, whereas 1.862-1.933Å for **4**. The Mn-N_i bond distances are: 2.063-2.30Å for **2**, 2.091-2.277Å (**A**) and 2.087-2.252Å (**B**) for **3** whereas 2.082-2.310Å for **4**. Some selected bond distances and angles for complexes **2-4** are summarized in **Table 2**. The non-covalent interactions e.g. hydrogen bonding, π···π and C–H···π stacking have been taken into account to clarify the possible supramolecular topologies.

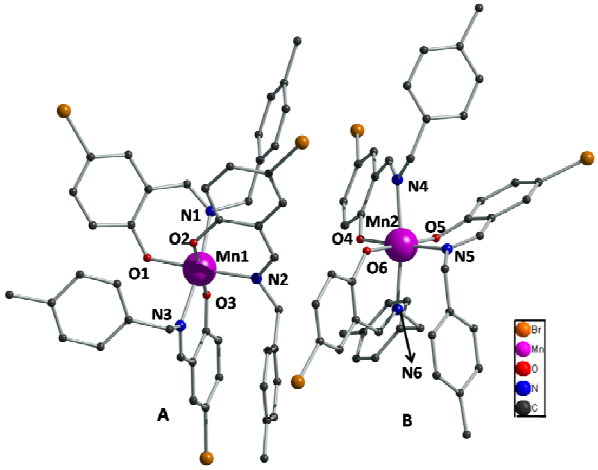

Fig. 2: The molecular view of complex **3**. All H-atoms are omitted for clarity.

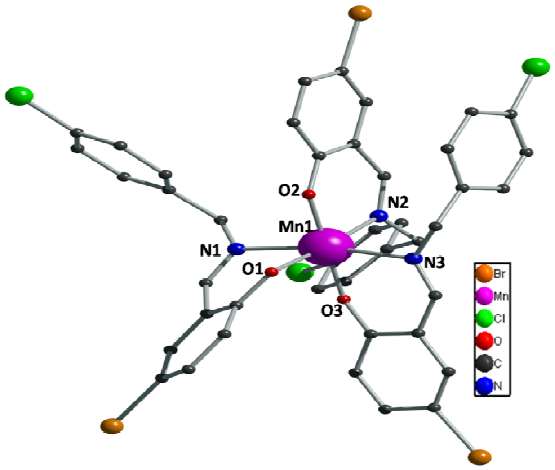

Fig. 3: The molecular view of complex **4**. All H-atoms are omitted for clarity.

In complex **2** the supramolecular interactions between: (i) aromatic hydrogen and one phenoxido oxygen (green dotted) (ii) π(aromatic)•••π(aromatic) (magenta dotted lines) and (iii) C–H•••π (green dotted lines) lead to the formation of supramolecular 1D chains along the crystallographic *c* axis (**Fig. 4**) and these 1D chains are further extended to 2D network (**Fig. S9**) via inter-locking Br···H interactions among themselves in the crystallographic *ab* plane. Similarly, complex **3** exhibits the same supramolecular topologies (**Fig. 5** and **S10**) via hydrogen bonding as well as C–H···π interactions in crystallographic *bc* plane. The hydrogen bonding (Br···H and Cl···H) and C–H···π interactions for complex **4** also play a crucial role for the formation of H-bonded supramolecular network (**Fig. S11**).

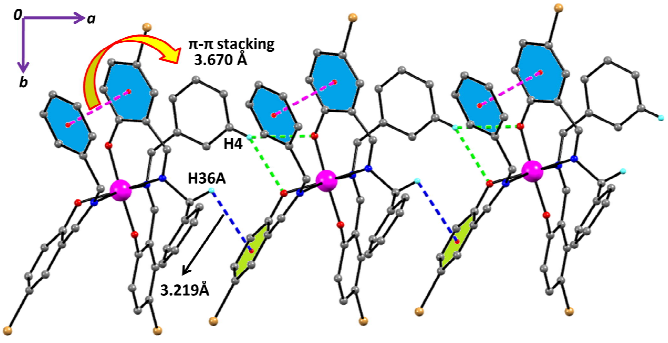

Fig. 4: The supramolecular interactions: H-bonding (green dotted lines), CH···π(phenyl) (blue lines) and π(phenyl)···π(phenyl) (magenta lines) are combined to form 1D network along crystallographic *c*-axis in **2**. All H-atoms except those involved in interactions are omitted for clarity.

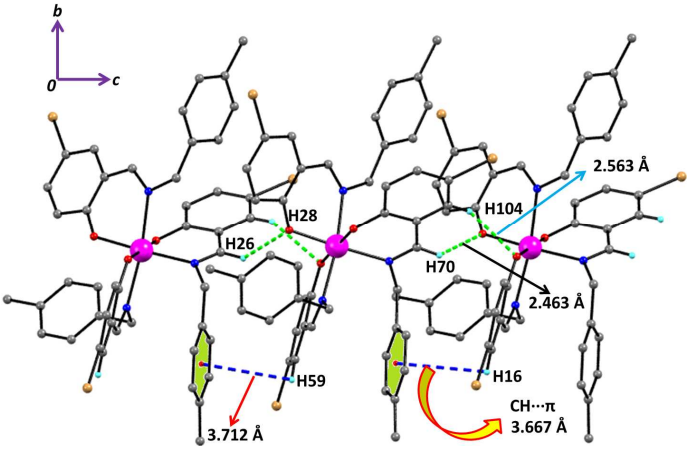

Fig. 5: The supramolecular interactions: H-bonding (green dotted line), CH···π (phenyl) (blue dotted line) are combined to form 1D framework along crystallographic *bc* plane in **3**.

Table 2. Selected bond distances and bond angles of complexes **2**-**4**.

2		**3**		**4**	
Mn1–O1	1.858(3)	Mn1–O2	1.909(8)	Mn1–O1	1.866(5)
	1.931(3)	Mn1–N2	2.277(10)	Mn1–O2	1.934(6)
Mn1–O2					
Mn1–O3	1.879(3)	Mn1–O3	1.877(6)	Mn1–O3	1.862(5)
Mn1–N1	2.300(3)	Mn1–N1	2.091(10)	Mn1–N1	2.281(7)
Mn1–N2	2.234(3)	Mn1–O1	1.905(6)	Mn1–N2	2.082(7)
Mn1–N3	2.063(3)	Mn1–N3	2.244(8)	Mn1–N3	2.310(7)
		Mn2–O5	1.893(6)		
		Mn2–O6	1.881(6)		
		Mn2–O4	1.930(8)		
		Mn2–N5	2.253(10)		
		Mn2–N6	2.245(10)		
		Mn2–N4	2.087(10)		
2		**3**		**4**	
O1–Mn1–O2	90.63(12)	O1–Mn1–O2	91.2(3)	O1–Mn1–O2	88.1(2)
O1–Mn1–O3	175.94(13)	O1–Mn1–O3	178.5(3)	O1–Mn1–O3	179.8(3)
O1–Mn1–N1	87.57(13)	O1–Mn1–N1	90.4(3)	O1–Mn1–N1	94.3(2)
O1–Mn1–N2	86.65(13)	O1–Mn1–N2	91.4(3)	O1–Mn1–N2	88.9(3)
O1–Mn1–N3	90.03(14)	O1–Mn1–N3	86.8(3)	O1–Mn1–N3	95.6(3)
O2–Mn1–O3	90.40(13)	O2–Mn1–O3	89.7(3)	O2–Mn1–O3	91.8(2)
O2–Mn1–N1	82.65(12)	O2–Mn1–N1	177.4(3)	O2–Mn1–N1	92.2(3)
O2–Mn1–N2	95.26(12)	O2–Mn1–N2	83.6(3)	O2–Mn1–N2	175.1(3)
O2–Mn1–N3	170.65(13)	O2–Mn1–N3	88.8(3)	O2–Mn1–N3	83.1(3)
O3–Mn1–N1	96.46(14)	O3–Mn1–N1	88.8(3)	O3–Mn1–N1	85.5(2)
O3–Mn1–N2	89.35(14)	O3–Mn1–N2	87.5(3)	O3–Mn1–N2	91.2(3)
O3–Mn1–N3	89.60(15)	O3–Mn1–N3	94.5(3)	O3–Mn1–N3	84.6(2)
N1–Mn1–N2	173.83(15)	N1–Mn1–N2	94.3(3)	N1–Mn1–N2	91.9(3)
N1–Mn1–N3	88.07(12)	N1–Mn1–N3	93.4(3)	N1–Mn1–N3	168.9(2)
N2–Mn1–N3	94.09(13)	N2–Mn1–N3	172.1(3)	N2–Mn1–N3	93.3(2)
		O5–Mn2–N6	87.2(3)		
		O6–Mn2–N4	88.5(3)		
		O6–Mn2–N5	87.8(3)		
		O6–Mn2–N6	93.5(3)		
		N4–Mn2–N5	94.2(3)		
		N4–Mn2–N6	93.7(3)		
		N5–Mn2–N6	172.0(3)		
		O4–Mn2–O5	91.0(3)		
		O4–Mn2–O6	89.8(3)		
		O4–Mn2–N4	177.4(3)		
		O4–Mn2–N5	83.8(3)		
		O4–Mn2–N6	88.4(3)		
		O5–Mn2–O6	178.9(3)		

Table 3. Summary of electronic spectra of Mn(III) complexes in DCM.

Complexes	λ_{max} (nm)	ε (dm^3 mol^{-1} cm^{-1}) x10^4	λ_{max}(nm)	ε (mol^{-1} dm^3 cm^{-1}) x 10^5
1	389	6.82	324	**1.32**
2	385	1.67	327	**0.38**
3	388	1.06	329	**0.20**
4	**389**	**2.69**	**328**	**0.43**

Electronic Spectra of Complexes:

The electronic spectra of all the four complexes were recorded in DCM, the details of which are incorporated in **Table 3**. Bands at ~333 and 389 nm correspond to the LMCT transitions (**Fig. 6**).[44]

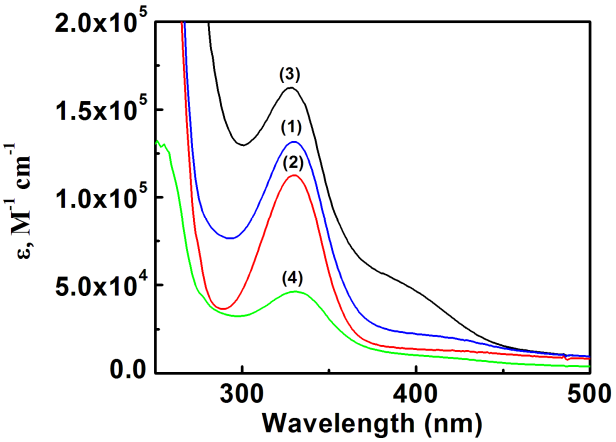

Fig 6. Electronic Spectra of manganese(III) complexes **1-4** in DCM. Conditions are given in **Table 3**.

Catecholase Activity

General Features:

The reaction of excess 3,5-ditertiarybutyl catechol (3,5-DTBC) with [**Mn(L^i)$_3$**] in DCM leads to the formation of 3,5-ditertiarybutyl quinone (3,5-DTBQ) as shown in equation (1). **Fig. 7** and **Figs. S12, S13** show time resolved spectra of the reaction of Mn(III) complexes (**1-4**) with 3,5-DTBC. When the complexes, **1-4** (~1.0 x 10^{-5} M) were treated with 3,5-DTBC in DCM, under aerobic conditions there was a gradual increase in absorbance at 403 nm, characteristics of the formation of 3,5-DTBQ.

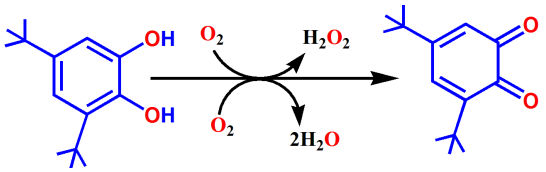

(1)

Kinetics

The formation of 3,5-DTBQ was monitored with time at a wavelength of ~ 400 nm (**Fig. 7**). The observed rate constants (k_i) were extracted by the initial rate method. Plots of k_i vs. [3,5-DTBC] gave non-linear curve of decreasing slope (**Fig. 8**) which are best described by equation (2) . A reasonable rate law can be derived as described in equation (3), where V = initial rate constant (k_i); [S] = concentration of the substrate, 3,5-DTBC; K_M = (k_2 + k_3)/k_1, Michaelis–Menten constant for the metal complex and V_{max} = maximum initial rate attained for a particular concentration of the metal complex in the presence of a large excess of the 3,5-DTBC. The liner form of the Michaelis–Menten equation is given in equation (4), known as Lineweaver–Burk Equation and corresponding fitting is shown in **Fig. S14**. Non-linear fitting of data to Michaelis-Menten equation (3) leads to the evaluation of V_{max}, K_M and K_{cat} = K_M/[complex] and all these parameters are listed in **Table 4**.

$$C + S \underset{k_{-1}}{\overset{k_1}{\rightleftharpoons}} CS \underset{k_{-2}}{\overset{k_2}{\rightleftharpoons}} C + P \qquad (2)$$

$$V = \frac{V_{max}[S]}{K_M + [S]} \qquad (3)$$

$$\frac{1}{V} = \frac{K_M}{V_{max}}\frac{1}{[S]} + \frac{1}{V_{max}} \qquad (4)$$

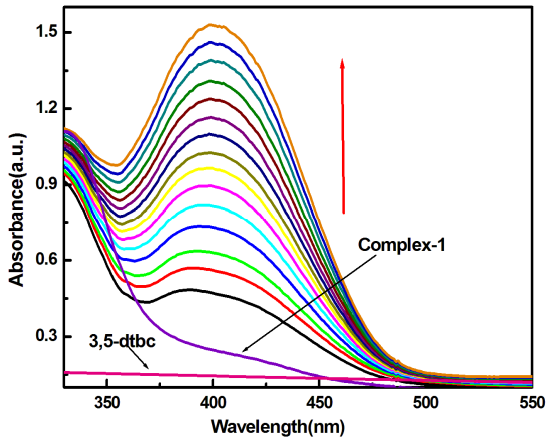

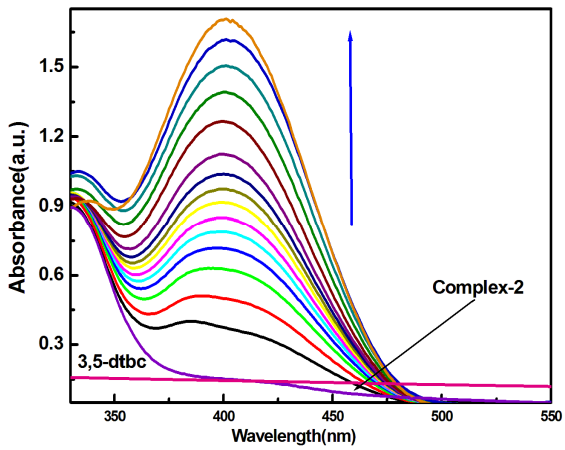

Fig. 7. Time-resolved spectra for the reaction of **1** and **2** with 5-DTBC in DCM.

Table 4. Summary of catecholase activity of **1**- **4** with 3,5-ditert-iarybutyl catechol in DCM. Conditions: [**c**] = 1.0 x 10^{-5} M.

Complex	10^4 x K_M	10^3 x V_{max} (M s^{-1})	K_{cat} (s^{-1})
1	1.79 ± 0.28	9.84 ± 3.27	17.9
2	3.48 ± 0.48	5.69 ± 0.22	34.8
3	1.70 ± 0.63	3.39 ± 0.27	17.0
4	2.51 ± 0.45	7.51 ± 0.33	25.1

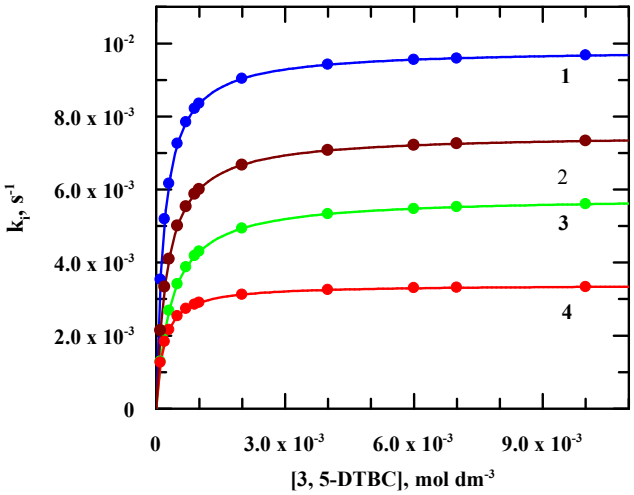

Fig. 8. Plots of k_i vs. [3, 5-ditertiarybutyl catechol] for the reaction of 3,5-DTBC with molecular oxygen catalyzed by manganese(III) complexes.

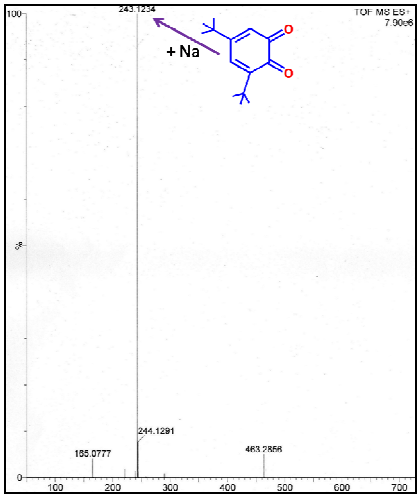

Fig 9. ESI-MS^+ (m/z) spectrum for the ultimate catecholase product during the reaction of **2** with 3, 5-DTBC.

Table 5. Catalytic Activity of Synthetic Catecholase Mimic

Compound	K_{cat} (h^{-1})	10^4 x K_M (M)	k_{cat}/K_M ($s^{-1}M^{-1}$)	ref
1	$6.44x10^4$	1.79	9.84	This work
2	$1.25x10^5$	3.48	5.69	This work
3	6.12×10^4	1.70	3.39	This work
4	9.04×10^4	2.51	7.51	This work
$[Mn(bpia)(OAc)(OCH_3)](PF_6)$	86	15.0	16	21
$[Mn(bipa)(OAc)(OCH_3)](PF_6)$	101	12.0	23	21
$[Mn(bpia)(Cl)_2](ClO_4)$	230	13.0	49	21
$[Mn(bipa)(Cl)_2](ClO_4)$	130	8.0	45	21
$[Mn(diclofenac)_2(H_2O)]^{a,b}$	225			46
$[Mn(tpa)_2](ClO_4)_2^{a,c}$	4			47
$[MnL^1(OOCH)(OH_2)]$	936.64	5.50	1.606×10^{-4}	25
$[MnL_2(OH_2)^2][Mn_2L_2^2(NO_2)_3]$	365.34	6.41	6.089×10^{-5}	"
$[Mn_2L_2^1(NO_2)_2]$	1432.74	49.17	2.388×10^{-4}	"
$[Mn^{III}_2Mn^{II}_4O_2(pyz)_2(C_6H_5CH_2COO)_{10}]_n$	2.547×10^3	1.75	7.076×10^{-5}	48
$Mn_2L^8Cl_4{\cdot}4H_2O$	3.60×10^3	9.00	1.00×10^{-4}	26

It is interesting to note that there are only few examples of where manganese complexes were claimed to display CO activities.[21,25,45-49] As for example, radical Mn(IV) complexes catalyzed the oxidation of 3,5-DTBC to 3,5-DTBQ in presence of molecular oxygen under mild conditions.[44→45] Some mononuclear Mn(III) complexes also found to favour the oxidation of catechol to quinone where direct involvement of Mn(III) was suggested.[45] **Table 5** displays the catalytic activities of some mononuclear Mn(III) as well as some multinuclear complexes. It is worth mentioning that our complexes showed the highest TON (K_{cat}, h^{-1}) for the catalytic oxidation of 3,5-DTBC to 3,5-DTBQ under mild

conditions by molecular oxygen and the existence of 3,5-DTBQ was identified from ESI-MS$^+$ (m/z) study (**Fig. 9**).

Magnetic study

Magnetic measurements have been carried out on all three mononuclear crystalline complexes **2–4**. Variable-temperature DC magnetic susceptibility (χ_M) of complexes **2–4** is investigated in the temperature range of 2–300 K under a magnetic field of 0.1 T. **Fig. 10** shows the variation of susceptibility in the form of $\chi_M T$ vs. T. The observed $\chi_M T$ values (2.95 and 2.65 cm^3 K mol^{-1}) for complexes **2** and **3** at 300K are close to the value obtained for uncoupled high spin S = 2 Mn(III) system (g = 2), while the same is quite low for complex **4** (1.21 cm^3 K mol^{-1}). Upon lowering the temperature for complexes **2** and **3**, the $\chi_M T$ product remains almost constant between 300 to 25 K and then decreases sharply to lower temperature regime down to 2K, signifying the presence of magnetic anisotropy (zero-field splitting). For complex **4**, the $\chi_M T$ product starts increasing from 300 to 25K and follows the same path at lower temperatures similar to complexes **2** and **3**. This anomalous behavior is due to the presence of strong supramolecular π•••π stacking interaction (intermolecular distance: 3.890 Å) in complex **4** which is weak in complex **3** and almost absent in complex **2**. This mediates the ferromagnetic exchange coupling (+ 0.16 cm^{-1}) between the two Mn(III) ions of the adjacent mononuclear units in complex **4**. The above susceptibility behavior is fitted using the following axial spin Hamiltonian (5).

$$H = g_1\beta\hat{H}S_1 + g_2\beta\hat{H}S_2 - 2JS_1S_2 + D_1\left[\hat{S}_{1z}^{\ 2} - \tfrac{1}{3}S_1(S_1+1)\right] + D_2\left[\hat{S}_{2z}^{\ 2} - \tfrac{1}{3}S_2(S_2+1)\right] \quad (5)$$

where, the specific terms have their usual meaning.

Weak intermolecular interaction (J) acting between two Mn(III) ions is incorporated in the expression (5) with zero field splitting (D) parameter to obtain the best fit parameters for g (Lande factor) and D (ZFS). The $\chi_M T$ data of the complexes were fitted assuming the same values of Lande g factors (g_1 and g_2) and the ZFS terms (D_1 and D_2) for the two exchange spin systems (S_1 and S_2). The magnetization data were fitted by taking the same g values obtained from the fitted plots of $\chi_M T$ vs. T (**Fig. 11** and **Fig. S15, S16**). This also leads to the same values of exchange and ZFS parameters, summarized in Table 6. In each case, the best fitted curve was obtained by the negative values of zero-field splitting (D) parameter.

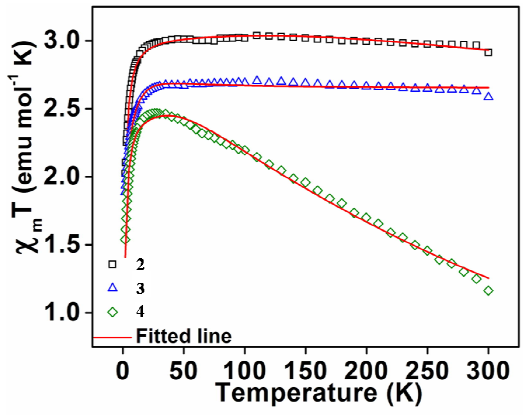

Fig.10: The variation of $\chi_M T$ (experimental points) with temperature for the three complexes **2**, **3** and **4**. Solid lines represent the theoretical curve and the points are the experimental data.

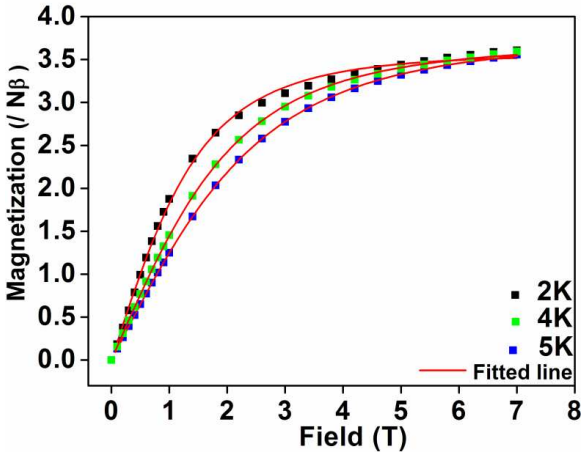

Fig. 11: M vs. H plots collected at 2, 4 and 5 K for complex **2**. Solid lines represent the theoretical curve and the points are the experimental data.

Table 6. Results of fitting of dc magnetic data and comparison with related systems.

Complex	D (cm^{-1})	J (cm^{-1})	g	10^4 x R^2
Mn(L^2)$_3$ (2)	– 2.96	– 0.08	1.98	1.89
Mn(L^3)$_3$ (3)	– 3.51	– 0.06	1.97	3.78
Mn(L^4)$_3$ (4)	– 3.72	+ 0.16	1.98	5.34
[Mn(dbm)$_3$][a]	-4.52		2.03	1.30
[Mn(dbm)$_2$(DMSO)$_2$](ClO$_4$)[a]	-3.42		1.92	4.10
[Mn(dbm)$_2$(py)$_2$](ClO$_4$)[a]	-4.46		1.97	0.47

Estimated errors: D (= ±0.02), J (= ±0.01); g (= ±0.01). [a]ref. 49. Dbm = dibenzoylmethane.

Table 6 displays ZFS values (D) for some recently reported octahedral Mn(III) complexes along with our results. The large negative D values are consistent with the Jahn–Teller axis elongation of the octahedral geometry.

Conclusion

We have synthesized four mononuclear Mn(III) complexes of bidentate Schiff base ligands out of which three (2-4) were characterized structurally and found to have octahedral geometries which showed excellent catechol oxidase activity with very high, probable the highest, turn over number (TON) of the so far reported Mn(III) complexes. Another interesting aspect of this study is that these complexes being in regular octahedral geometry and devoid of any labile ancillary ligand which encourages the coordination of catechol to the metal center also showed CO activity. Cryomagnetic studies on complexes **2-4** gives very high negative ZFS values, comparable to recently reported values.

Acknowledgement

Financial support from CSIR (Ref. 02(2490)/11/EMR-II) and UGC [39-735/2010(SR)], New Delhi, are gratefully acknowledged.

References

1 S. Mukhopadhyay, S. K. Mandal, S. Bhaduri and W. H. Armstrong, *Chem. Rev.,* 2004, **104**, 3981.

2 B. Zhou, R. Tao, S. Q. Shen and J. Q. Liang, *Phys, Rev. A*, 2002, **66**, 01030.

3 D. Gatteschi and R. Sessoli, *Angew. Chem. Int. Ed*., 2003, **42**, 268.

4 J. W. Whittaker, In *Metal Ions in Biological Systems*, ed. A. Sigel and H. Sigel, Marcel Dekker, New York, 2000, **37**, 587.

5 L. Que, Jr. and M. F. Reynolds, In *Metal Ions in Biological Systems*, ed. A. Sigel and H. Sigel, Marcel Dekker, New York, 2000, **37**, 505.

6 (*a*) Y. Kono and I. Fridovich, *J. Biol. Chem*., 1983, **258**, 6015; (*b*) W. F. Beyer, Jr. and I. Fridovich, *Biochemistry*, 1985, **24**, 6460.

7 (*a*) V. V. Barynin, A. A. Vagin, W. R.Melik-Adamyan, A. I. Grebenko, S. V. Khangulov, A. N. Popov, M. E. Andrianova and B.K. Vainshtein, *Dokl. Akad. Nauk.*, 1986, **288**, 877; (*b*) V. V. Barynin, P. D. Hempstead, A. A. Vagin, S. V. Antonyuk, W. R. M. Adamyan, V. S. Lamzin, P. M. Harrison and P. J. Artymyuk, *J. Inorg. Biochem.*, 1997, **67**, 196.

8 G. S. Allgood and J. J. Perry, *J. Bacteriol*., 1986, **168**, 563.

9 I. Michaud-Soret, L. Jacquamet, N. Debaecker-Petit, L. Le Pape, V. V. Barynin and J. M. Latour, *Inorg. Chem.*, 1998, **37**, 3874.

10 A. J. Wu, J. E. Penner-Hahn and V. L. Pecoraro, *Chem. Rev*., 2004, **104**, 903.

11 G. Auling and H. Follmann, In *Metal Ions in Biological Systems*, ed. A. Sigel and H. Sigel, Marcel Dekker, New York, 1994, **30**, 131.

12 D. E. Ash, J. D. Cox and D. W. Christianson, In *Metal Ions in Biological Systems*, ed. A. Sigel and H. Sigel, Marcel Dekker, New York, 2000, **37**, 407.

13 M. U. Triller, W. Y. Hsieh, V. L. Pecoraro, A. Rompel and B. Krebs, *Inorg. Chem*., 2002, **41**, 5544.

14 K. A. Jørgensen, *Chem. Rev.,* 1989, **89**, 431.

15 M.J. Gunter and P. Turner, *Coord. Chem. Rev.,* 1991, **108**, 115.

16 T. Katsuki, *Coord. Chem. Rev.,* 1995, **140**, 189.

17 T. Katsuki and I. Ojima (Ed.*), Catalytic Asymmetric Synthesis, second ed.,* Wiley, New York, 2000, 287.

18 S. Majumder, S. Hazra, P. Biswas and S. Mohanta, *Polyhedron,* 2009, **28**, 2473.

19 V. L. Pecoraro, M. J. Baldwin and A. Gelasco, *Chem. Rev.,* 1994, **94**, 807.

20 A. J. Wu, J. E. Penner-Hahn and V. L. Pecoraro, *Chem. Rev.,* 2004, **104**, 903.

21 M. U. Triller, D. Pursche, W. Y. Hsieh, V. L. Pecoraro, A. Rompel and B. Krebs, *Inorg. Chem*., 2003, **42**, 6274.

22 S. Mukherjee, T. Weyhermuller, E. Bothe, K. Wieghardt and P. Chaudhuri, *Dalton Trans*., 2004, 3842.

23 S. Mukherjee, E. Rentschler, T. Weyhermuller, K. Wieghardt and P. Chaudhuri, *Chem. Commun*., 2003, 1828.

24 S. Mukherjee, E. Rentschler, T. Weyhermüller, K. Wieghardt and P. Chaudhuri, *J. Chem. Soc., Chem. Commun.,* 2003, 1828.

25. P. Seth, M.G.B. Drew, A. Ghosh, *Journal of Molecular Catalysis A: Chemical* 2012,**365**,154– 161

26. K. S. Banu, T. Chattopadhyay, A. Banerjee, M.Mukherjee, S. Bhattacharya, G. K. Patra, E. Zangrando and D. Das, *Dalton Trans.*, 2009, 8755–8764.

27. P. Chakraborty, S. Majumder, A. Jana, S. Mohanta, *Inorg. Chim. Acta*, 2014, **410**, 65–75

28 A. Guha, K.S. Banu, A. Banerjee, T. Ghosh, S.Bhattacharya, E. Zangrando, D. Das,*J. Mol. Catal. A,* 2011,**338**, 51.

29 J. Kaizer, G. Barath, R. Csonka, G. Speier, L. Korecz, A. Rockenbauer, L. Parka˜ nyi,*J. Inorg. Biochem.,* 2008, **102**, 773.

30 J. Kaizer, R. Csonka, G. Barath, G. Speier, *Trans. Met. Chem.* 2007,**32**, 1047.

31 A. Majumder, S. Goswami, S.R. Batten, M.S.E. Fallah, J. Ribas, S. Mitra, *Inorg.Chim. Acta*, 2006, **359**, 2375.

32 K.S. Banu, T. Chattopadhyay, A. Banerjee, M. Mukherjee, A.S. Bhattacharya, G.K. Patra, E. Zangrando, D. Das, *Dalton Trans.,* 2009, 8755.

33 S. Mukherjee, T. Weyhermuller, E. Bothe, K. Wieghardt, P. Chaudhuri, *Dalton.Trans.,* 2004, 3842.

34 G. Blay, I. Fernandez, J.R. Pedro, R. Ruiz, T.T. Sanchez, E. Pardo, F. Lloret, M.C. Munoz, *J. Mol. Catal. A,* 2006, **250**, 20.

35 A. Jana, N. Aliaga-Alcalde, E. Ruiz and S. Mohanta*, Inorg. Chem.,* 2013, **52**, 7732.

36 J. Kaizer, R. Csonka, G. Baráth and G. Speier, *Trans. Met. Chem.,* 2007, **32**, 1047.

37 L. I. Simándi and T. L. Simándi, *J. Chem. Soc., Dalton Trans.,* 1998, 3275.

38 J. Krzystek, G.-J. Yeagle, J.-H. Park, R.-D. Britt, M.-W. Meisel, L.-C. Brunel, J. Telser, *Inorg. Chem.*, 2003, **42** , 4610.

39 J. Krzystek, A. Ozarowski, J. Telser, *Coord. Chem. Rev*., 2006, **250**, 2308.

40 J. Vallejo, A. Pascual-Álvarez, J. Cano, I. Castro, M. Julve, F. Lloret, J. Krzystek, G. D.Munno, D. Armentano, W. Wernsdorfer, R. Ruiz-García, E. Pardo, *Angew. Chem. Int. Ed.,* 2013, **52**, 14075.

41. B. J. Kennedy and K. S. Murray*, Inorg. Chem.,* 1985, **24**, 1552 and the references therein.

42. A. Altomare, M.C. Burla, M. Camalli, G.L. Cascarano, C. Giacovazzo, A. Guagliardi, A.G.G. Moliterni, G. Polidori, R. Spagna, *J. Appl. Crystallogr*., 1999, **32**,115.

43. SHELX97 – Programs for Crystal Structure Analysis (Release 97-2), G.M. Sheldrick, Institüt für Anorganische Chemie der Universität, Tamman strasse 4, D-3400 Göttingen, Germany, 1998.

44. A. Westphal, A. Klinkebiel, H.-M. Berends, H. Broda, P. Kurz, and F. Tuczek, *Inorg. Chem.,* 2013, **52**, 2372;

44. E.I. Solomon, U.M. Sundaram, T.E. Machonkin, *Chem. Rev*., 1996, **96**, 2563.

45. N. Kitajima, Y. Morooka, *Chem. Rev.,* 1994, **94**, 737.

46. D. Kovala-Demertzi, S. K.Hadjikakou, M. A. Demertzis and Y. Deligiannakis, *J. Inorg. Biochem.,* 1998, **69**, 223.

47. Y.Gultneh, A. Farooq, K. D. Karlin, S.Liu and J. Zubieta, *Inorg. Chim.Acta,* 1993, **211**, 171.

48. P. Kar, R. Haldar, C. J. Gómez-García and A. Ghosh, *Inorg. Chem*., 2012, **51**, 4265.

49 L. Chen, J. Wang, Y.-Z. Liu, Y. Song, X.-T. Chen, Y.-Q. Zhang, and Z.-L. Xue, *Eur. J. Inorg. Chem.,* 0000, 0–0, DOI:10.1002/ejic.201402964.